Electronic Supplementary Material (ESI) for Journal of Materials Chemistry A.

Synthesis of Three-Component Cu_2O/ZnO/Ag Nanocrystals Heterogeneous Photocatalysts with High Reactivity and Stability for Dye Reduction

Chih-Wu Chiang, Chieh-Yu Lai, and Su-Wen Hsu*

Department of Chemical Engineering, National Cheng Kung University, Taiwan

No. 1 University Road, East Dist., Tainan City 70101, Taiwan (R.O.C)

*E-mail: swhsu@gs.ncku.edu.tw ‡These authors contributed equally

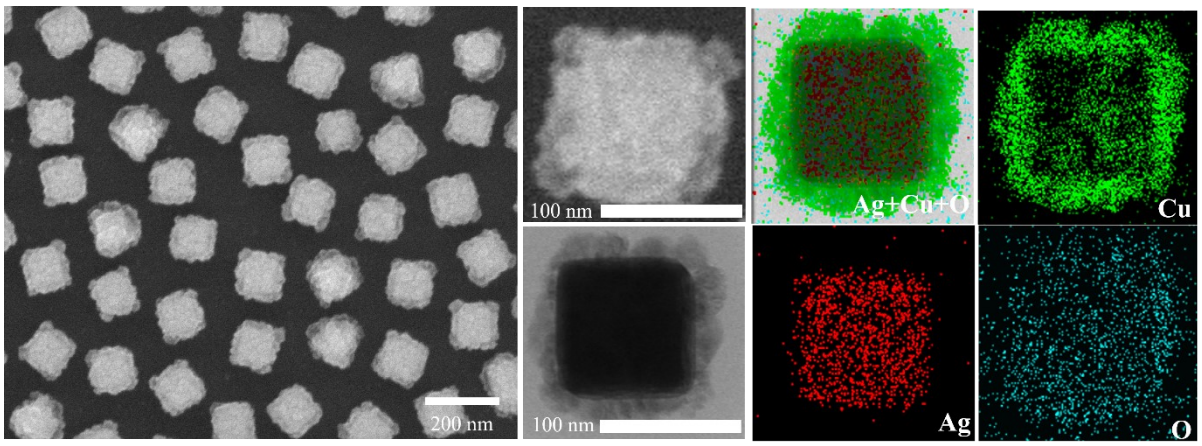

Figure S1 The morphology of Cu_2O-AgNC nanocrystals and component analysis. The SEM and HRTEM EDS mapping images show the uniform core-shell nanocrystal with an average Cu content of about 24.2 atomic%.

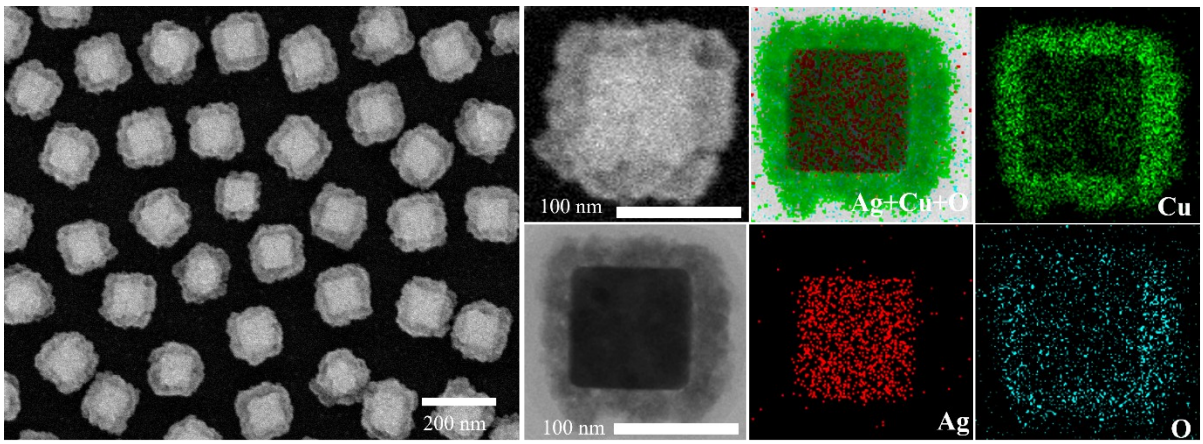

Figure S2 The morphology of Cu_2O-AgNC nanocrystals and component analysis. The SEM and HRTEM EDS mapping images show the uniform core-shell nanocrystal with an average Cu content of about 28.8 atomic%.

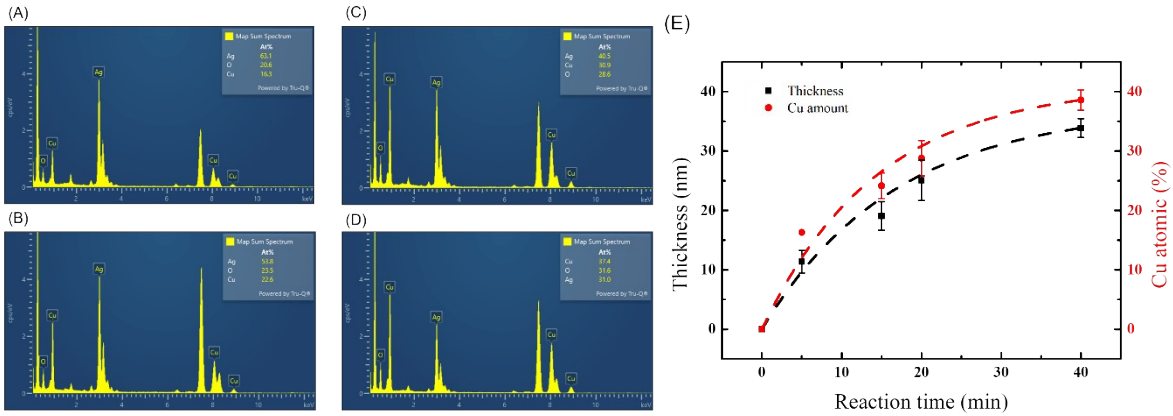

Figure S3 EDS analysis of the component of Cu_2O-AgNC with different reaction times. The average Cu content increased with reaction time: 16.3, 24.2, 28.8, and 38.6 atomic % as shown in (A)-(D), respectively. (E) The average thickness and Cu content of the Cu_2O layer varied with the reaction time. Here, the thickness of the Cu2O layer was calculated by analyzing of the SEM images.

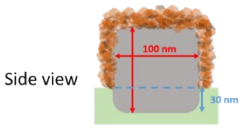

$$Cu_2O\ thickness = (\sqrt{Area_{Cu_2O}} - \sqrt{Area_{Ag}}) \div 2$$

$$V_{AgNC} = (100)^3\ (nm)^3$$

$$V_{Cu_2O} = (100 + 2 \times Cu_2O\ thickness)^2 \times (Cu_2O\ thickness + 70)$$

$$D_{Ag} = 10.49\ (^g/_{cm^3}) \qquad Mw_{Ag} = 107.87\ (^g/_{mol})$$

$$D_{Cu_2O} = 6\ (^g/_{cm^3}) \qquad Mw_{C\,u_2O} = 143.09\ (^g/_{mol})$$

$$\#\ of\ Ag\ atoms = V_{AgNC} \times D_{Ag} \div Mw_{Ag}$$

$$\#\ of\ Cu\ atoms = V_{Cu_2O} \times D_{Cu_2O} \div Mw_{C\,u_2O} \times 2$$

$$\frac{Cu\ atom\%}{Ag\ atom\%} = \frac{\#\ of\ Cu\ atoms}{\#\ of\ Ag\ atoms}$$

$$Porosity = 1 - \frac{\frac{\#\ of\ Cu\ atoms}{\#\ of\ Ag\ atoms}\ (EDS)}{\frac{\#\ of\ Cu\ atoms}{\#\ of\ Ag\ atoms}\ (calculation)}$$

Sample name	Thickness of Cu_2O (nm)	Ag content atomic (%) (EDS)	Cu content atomic (%) (EDS)	$\frac{\#\ of\ Cu\ atoms}{\#\ of\ Ag\ atoms}$ (EDS)	$\frac{\#\ of\ Cu\ atoms}{\#\ of\ Ag\ atoms}$ (calculation)	Porosity
Cu_2O-AgNC-I	11.4	63.1	16.3	0.258	0.455	0.433
Cu_2O-AgNC-II	19.1	51.4	24.2	0.470	0.864	0.456
Cu_2O-AgNC-III	25.1	43.2	28.8	0.667	1.247	0.465
Cu_2O-AgNC-IV	33.9	38.6	38.6	1	1.919	0.479

Figure S4 Theoretical calculation of porosity of Cu_2O-AgNC nanocomposites.

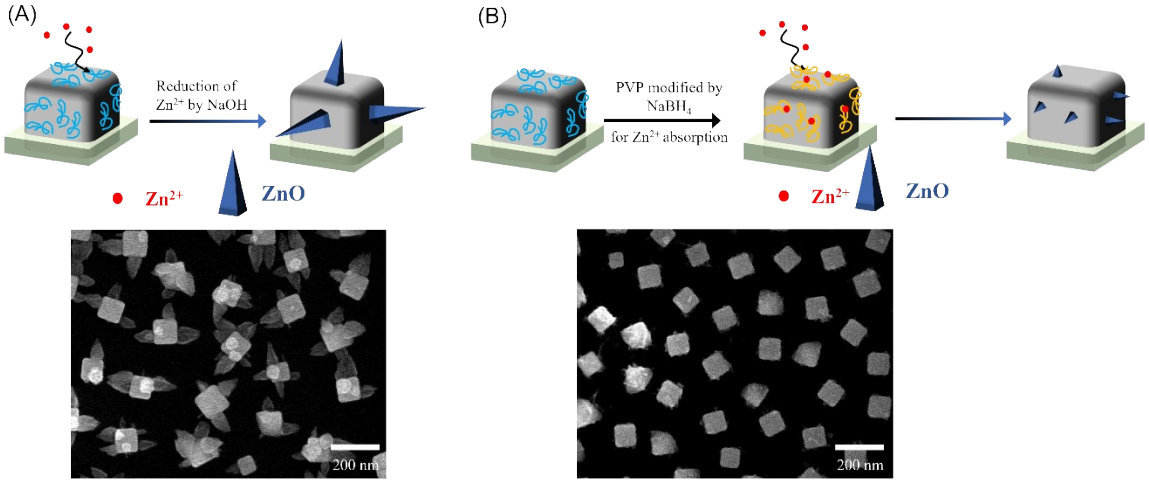

Figure S5 Different synthesis processes for ZnO-AgNC nanocrystal formation. (A) The reduction of Zn^{2+} ions on the surface of PVP-AgNC without $NaBH_4$ modification resulted in the non-uniform growth of ZnO as shown in the SEM image. (B) In the absence of NaOH, the reduction of Zn^{2+} ions on the surface of AgNC resulted in a decrease growth rate of ZnO as shown in the SEM image.

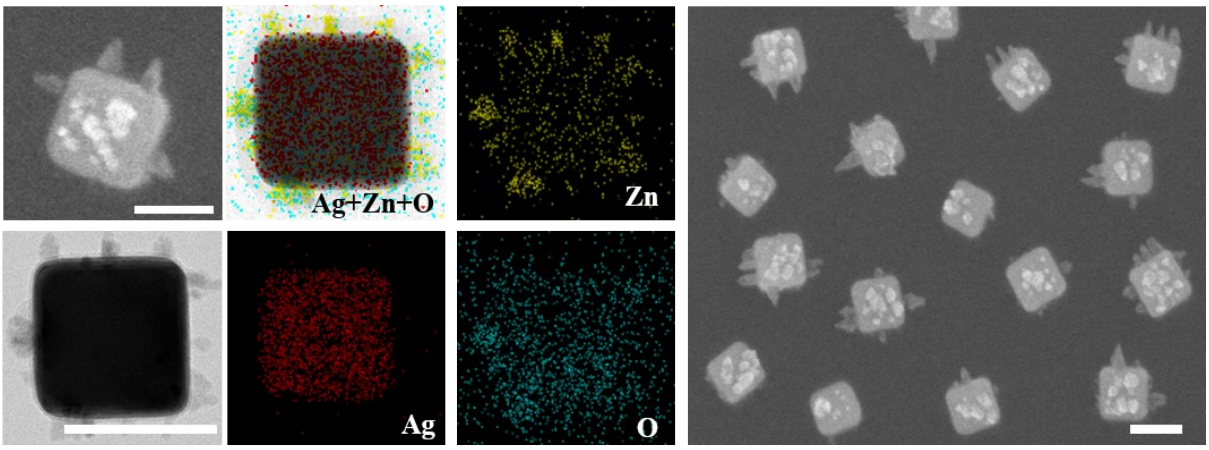

Figure S6 The morphology of ZnO-AgNC nanocrystals and component analysis. The SEM and HRTEM EDS mapping images show the uniform core-shell nanocrystal with an average Zn content of about 1.3 atomic%.

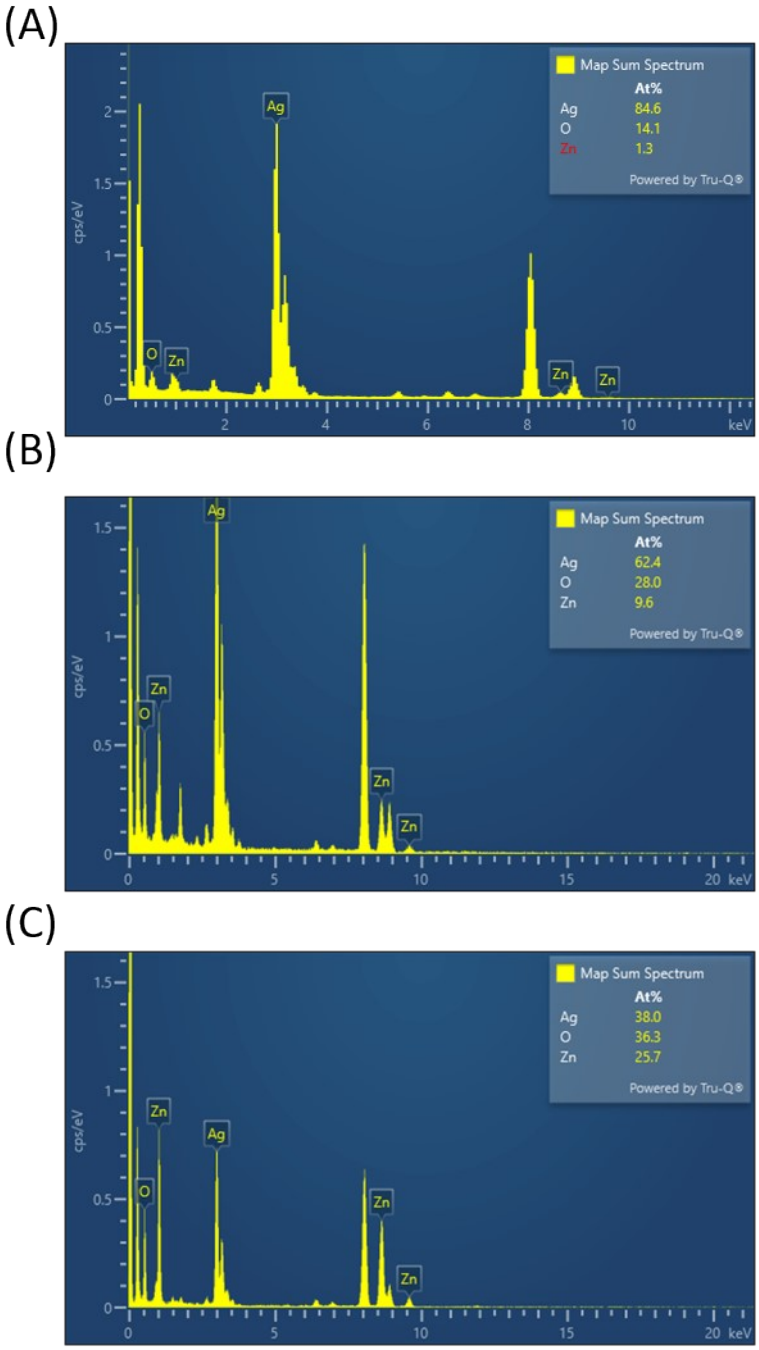

Figure S7 EDS analysis of the component of ZnO-AgNC with different reaction times. The average Zn content increased with reaction time: 1.3, 9.6, and 25.7 atomic % as shown in (A)-(C), respectively.

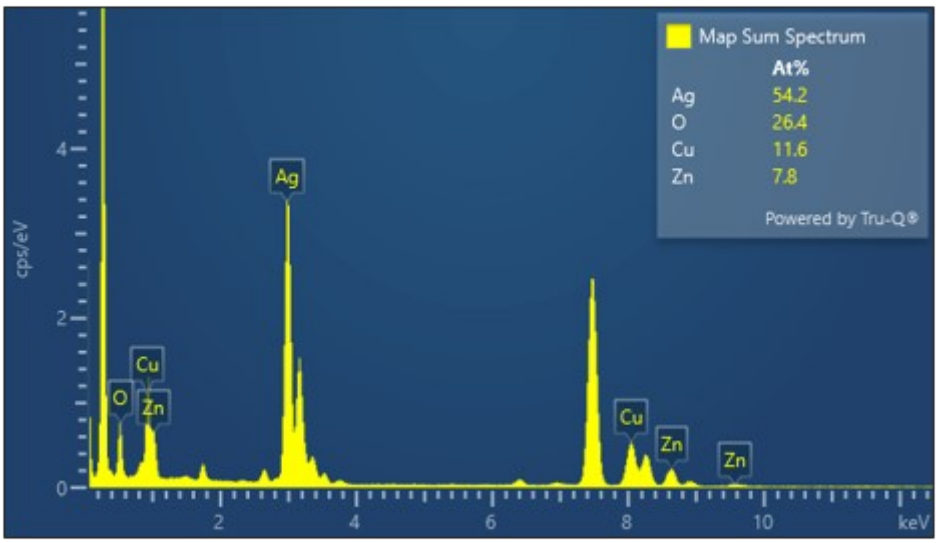

Figure S8 EDS analysis of the component of ZnO/Cu_2O-AgNC. The average Zn content is ~ 7.8 atomic % and Cu content is ~ 11.6 atomic%.

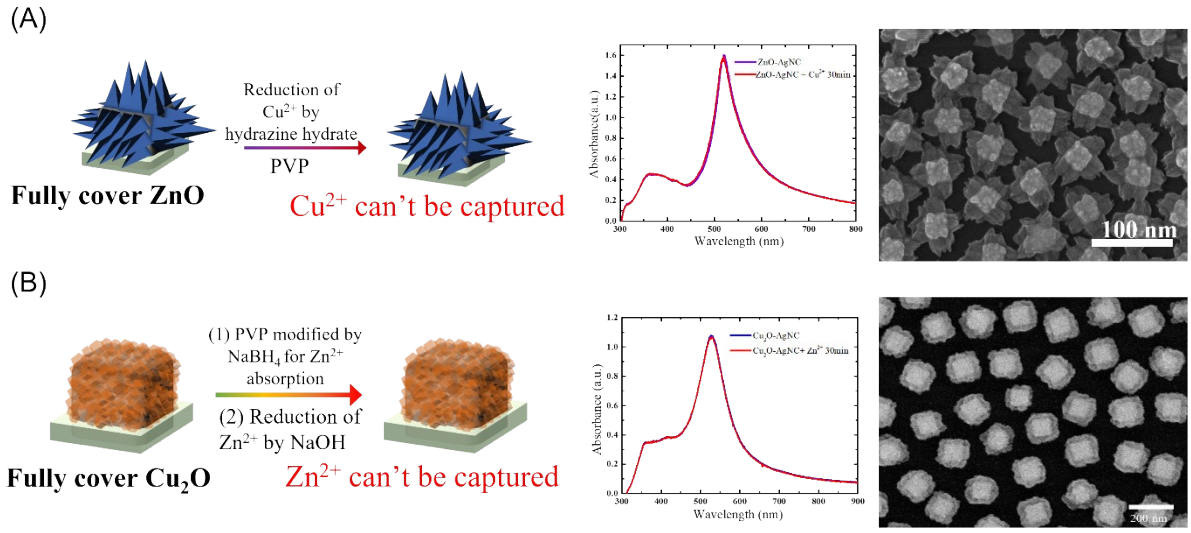

Figure S9 Different synthesis processes for ZnO/Cu_2O-AgNC nanocrystal formation. (A) The reduction of Cu^{2+} ions on AgNC nanocrystals with fully covered ZnO resulted in no formation of Cu_2O as shown in the SEM image. (B) The reduction of Zn^{2+} ions on AgNC nanocrystals with fully covered Cu_2O resulted in no formation of ZnO as shown in the SEM image. The corresponding extinction spectra of the ZnO/Cu_2O-AgNC nanocrystal synthesis process showed no change in the spectra during the reaction time.

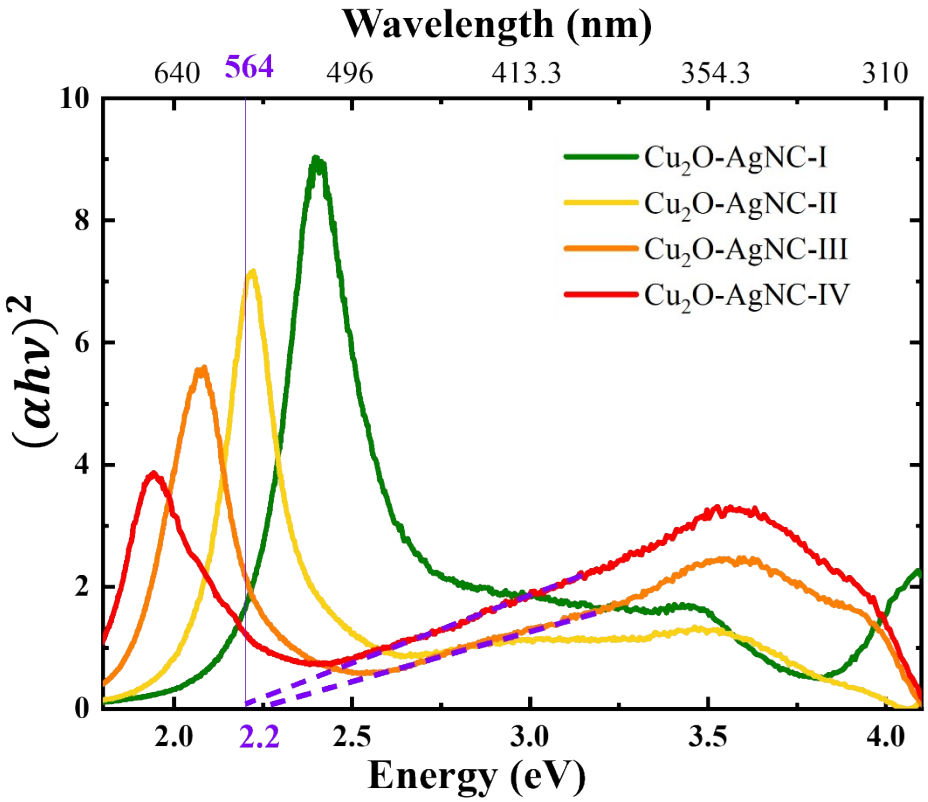

Figure S10 The energy gap of Cu_2O-AgNC nanocrystals can be calculated by $(\alpha hv)^2$-energy plot. Cu_2O-AgNC nanocrystals with different Cu contents showed an energy gap of about 2.2 eV, corresponding to 564 nm yellow light. And the absorption curves (yellow curve and green curve) of nanocrystals with lower Cu_2O content originate from the overlap between the plasmonic resonance peak of AgNC and the band gap absorption of Cu_2O, which make it impossible to predict the energy gap of Cu_2O using $(\alpha hv)^2$-energy plot.

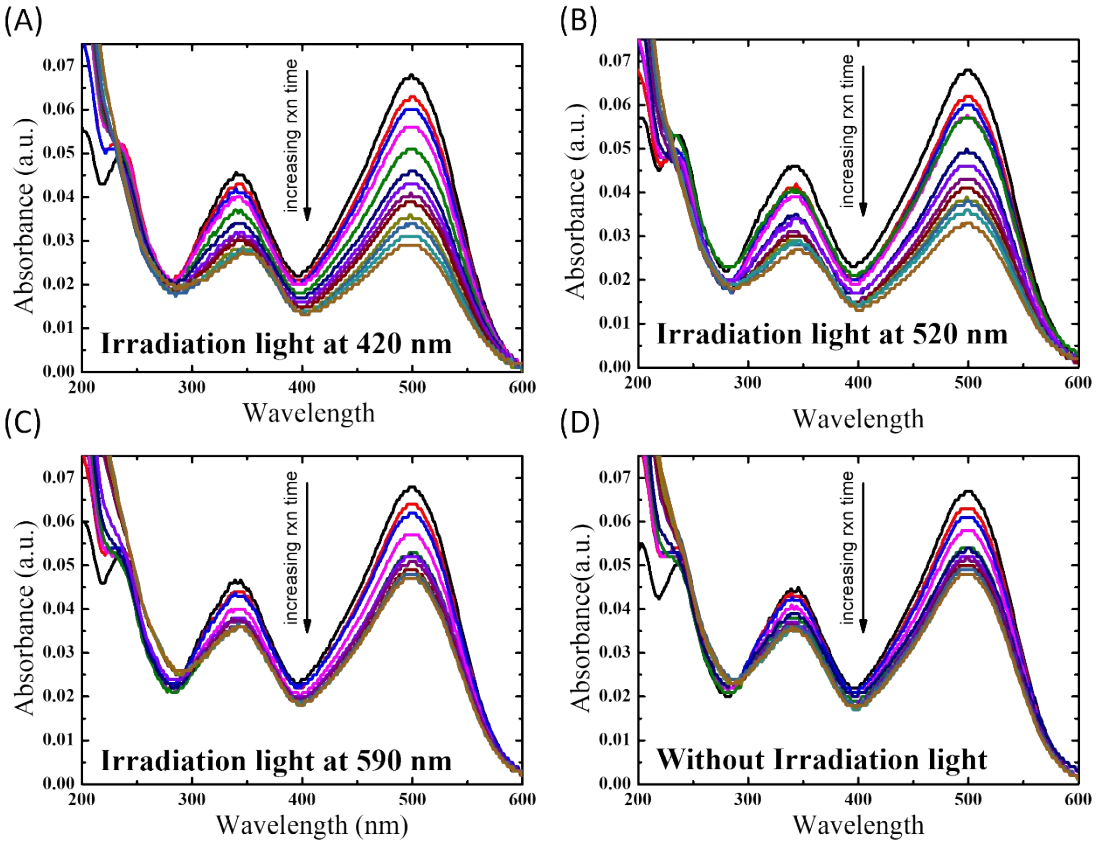

Figure S11 Cu_2O-AgNC nanocrystals with Cu content 16.3 atomic% were used as photocatalysts to reduce Congo red reduction under different irradiation. Changes in the Uv-Vis spectra of Congo red solution during reduction under irradiation light at (A) 420 nm, (B) 520nm, and (C) 590 nm compared to non-irradiation (D).

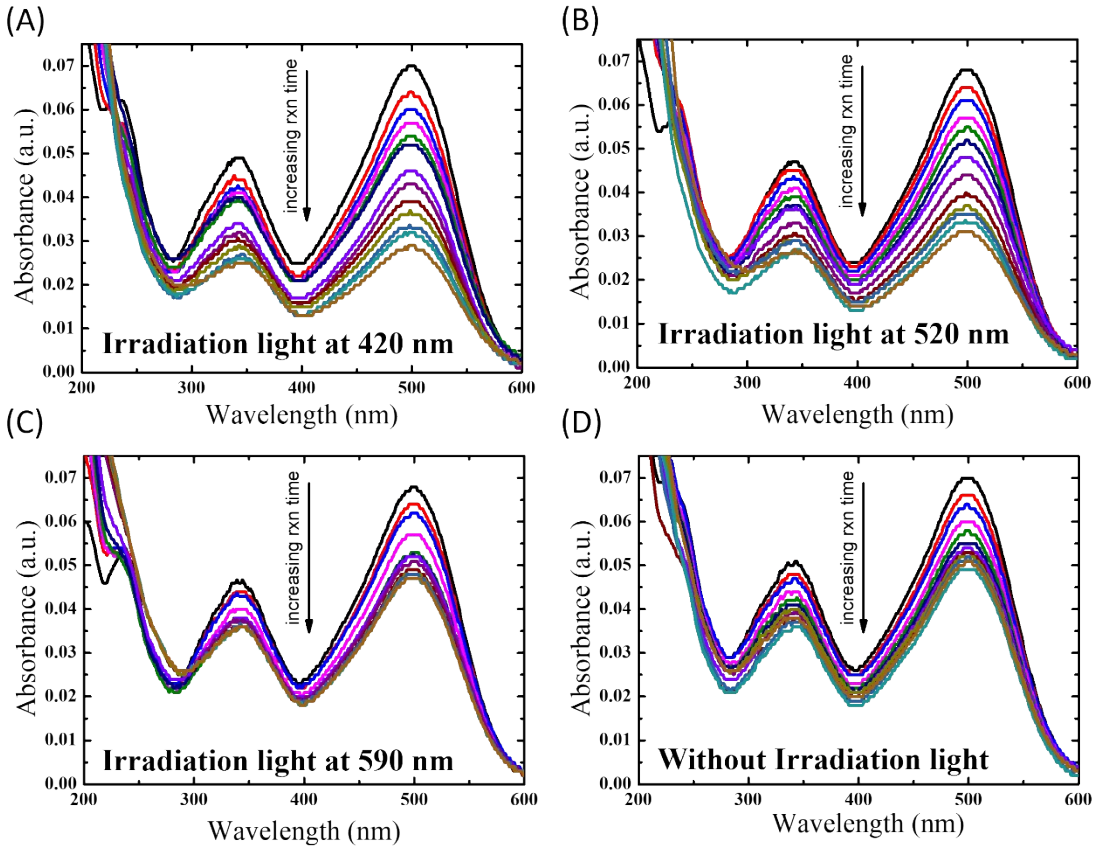

Figure S12 Cu_2O-AgNC nanocrystals with Cu content 24.2 atomic% were used as photocatalysts to reduce Congo red reduction under different irradiation. Changes in the Uv-Vis spectra of Congo red solution during reduction under irradiation light at (A) 420 nm, (B) 520nm, and (C) 590 nm compared to non-irradiation (D).

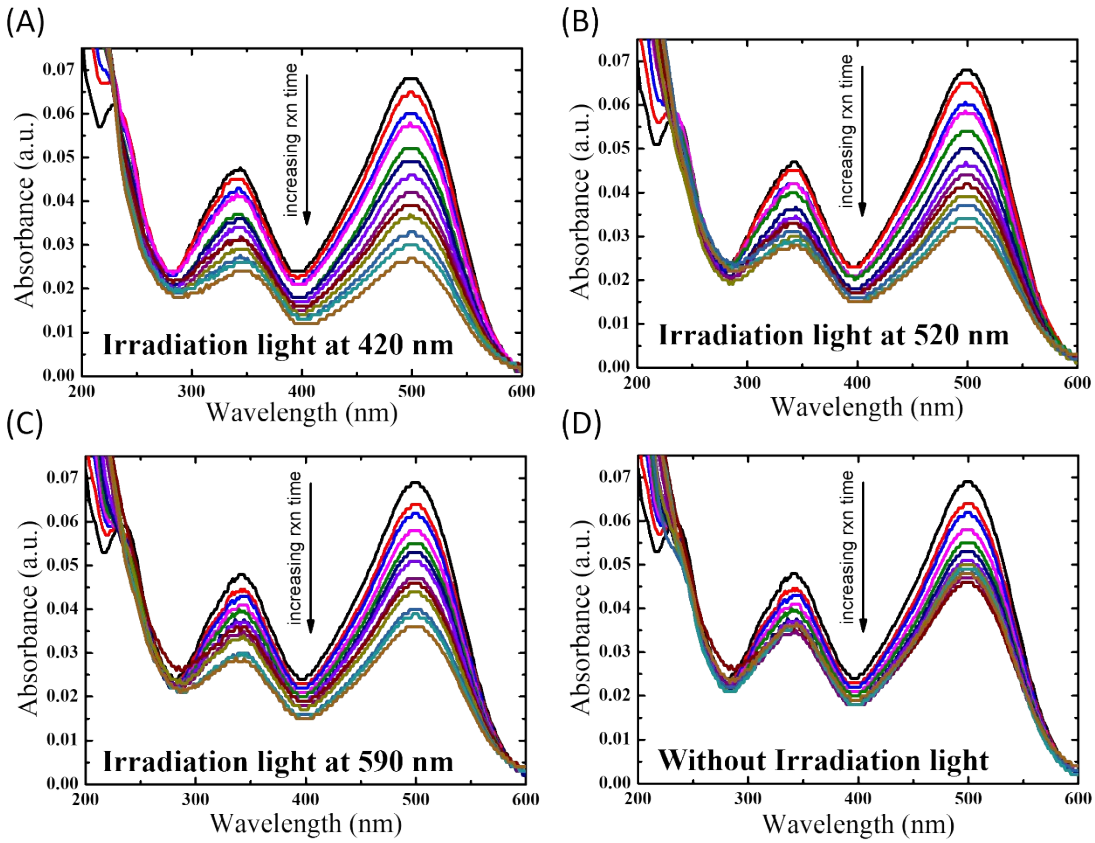

Figure S13 Cu_2O-AgNC nanocrystals with Cu content 28.8 atomic% were used as photocatalysts to reduce Congo red reduction under different irradiation. Changes in the Uv-Vis spectra of Congo red solution during reduction under irradiation light at (A) 420 nm, (B) 520nm, and (C) 590 nm compared to non-irradiation (D).

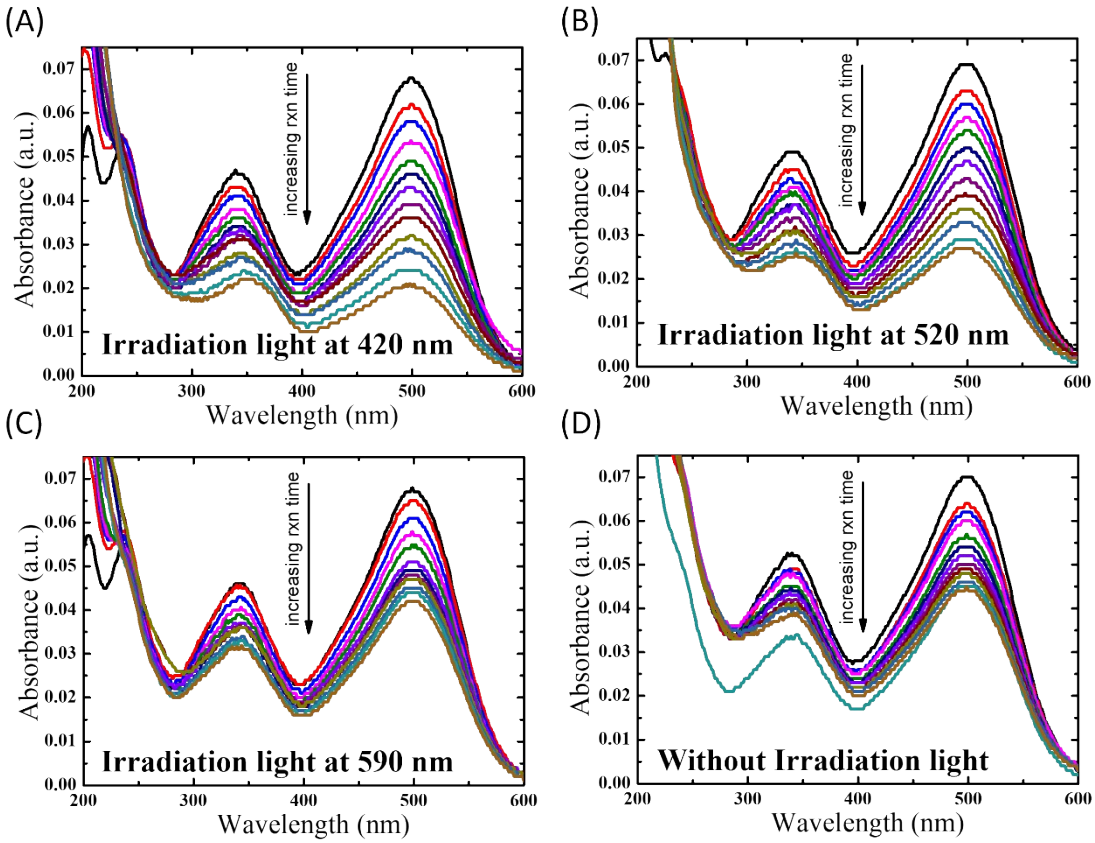

Figure S14 Cu_2O-AgNC nanocrystals with Cu content 38.6 atomic% were used as photocatalysts to reduce Congo red reduction under different irradiation. Changes in the Uv-Vis spectra of Congo red solution during reduction under irradiation light at (A) 420 nm, (B) 520nm, and (C) 590 nm compared to non-irradiation (D).

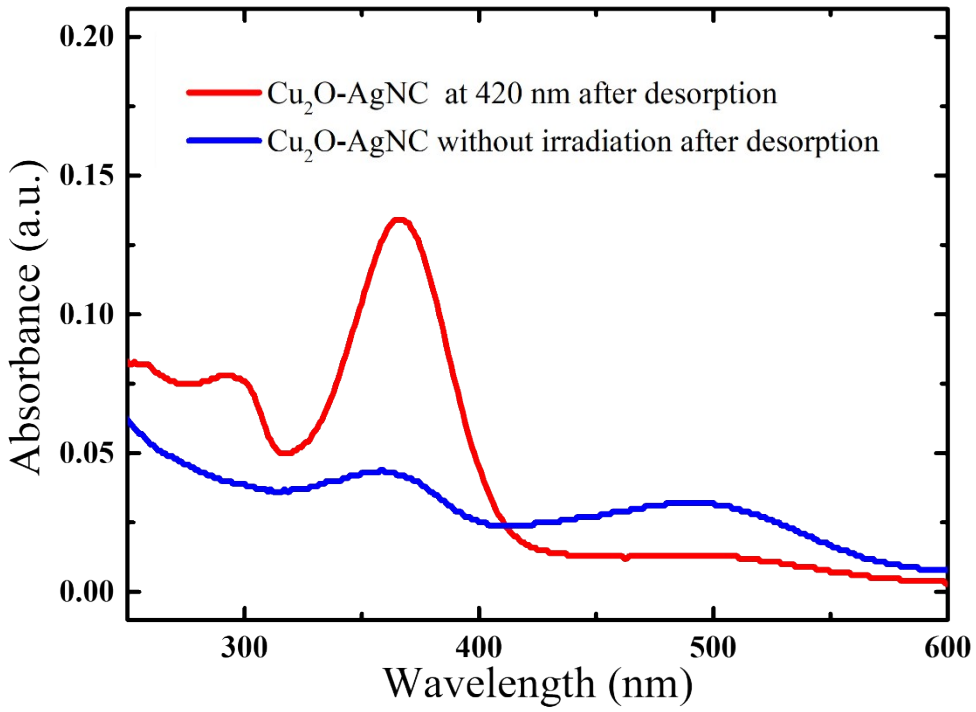

Figure S15 Desorption of Conge red and reduced products from Cu_2O-AgNC nanocrystals after Congo reduction reaction occurred on Cu_2O-AgNC nanocrystals. The Cu_2O-AgNC nanocrystals after the reduction reaction was placed in DI water for 24 hours, and then used the absorption peaks of Congo red and reduced products (naphthalene at ~340 nm) in aqueous solution were detected by Uv-Vis spectroscopy. Congo red reduction does not occur in the absence of external irradiation, resulting in only the Congo red absorption peaks in Uv-Vis spectrum (blue curve). However, Congo red can be reduced under external irradiation and resulting in the reduced product having an absorption peak at 365 nm (red curve).

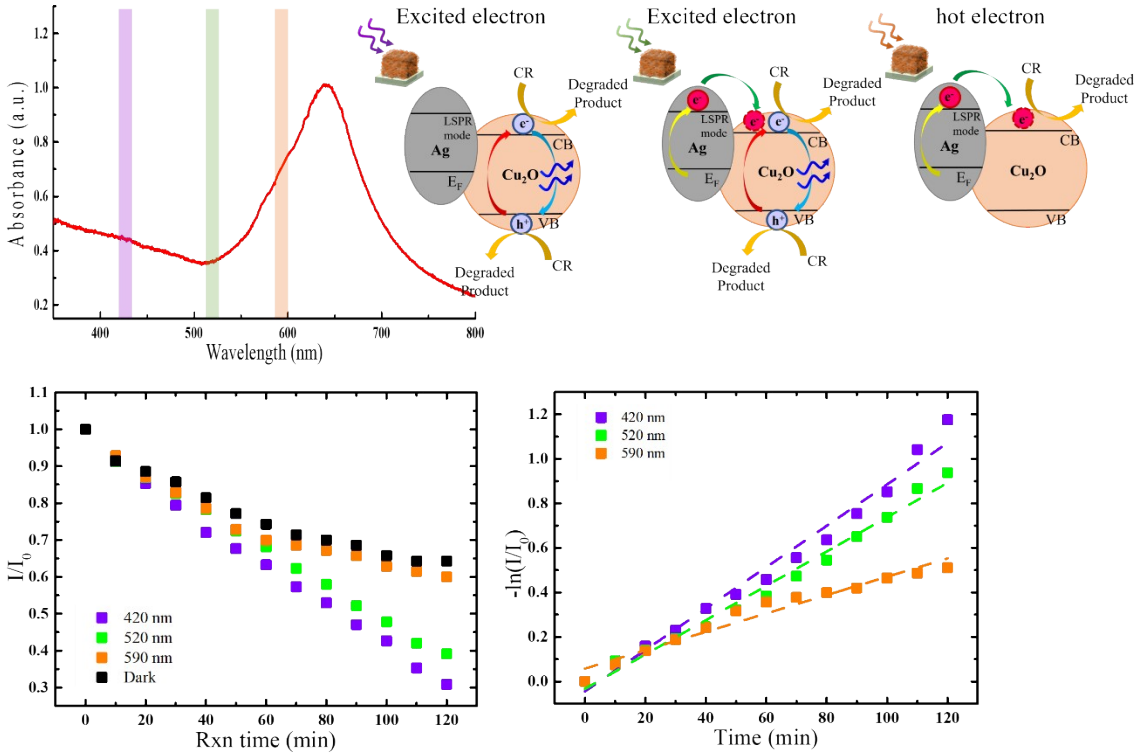

Figure S16 Photocatalytic performance of Cu_2O-AgNC nanocrystal for reduction of Congo red under different irradiation wavelengths. Green (520 nm) and violet (420 nm) light generate excited electrons for the reduction of Congo red. Orange light (590 nm) generates plasmonic hot electrons for the reduction of Congo red reduction.

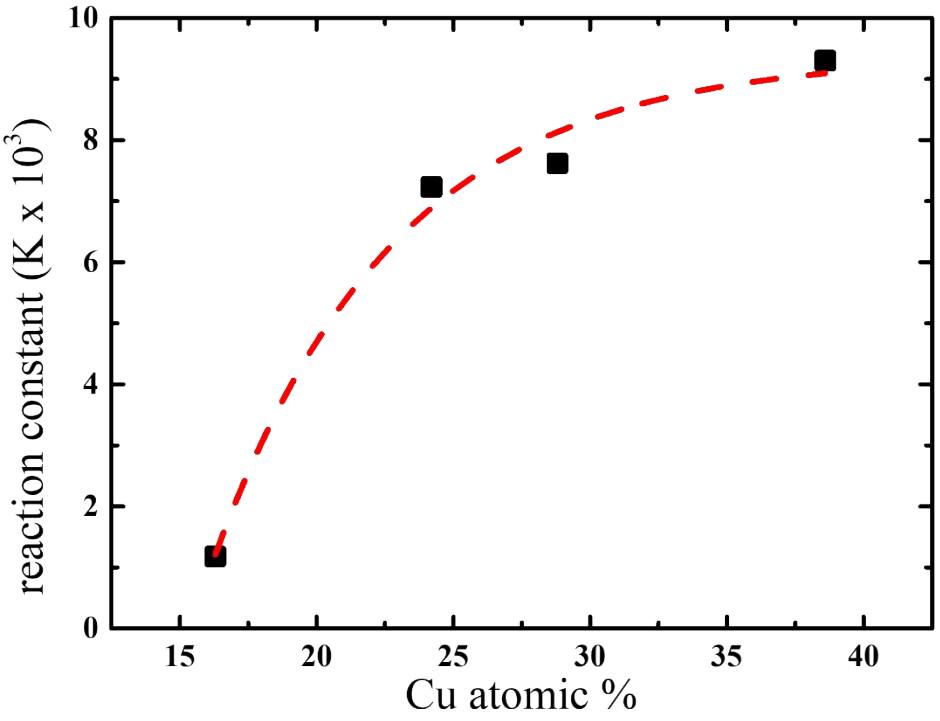

Figure S17 Effect of the Cu content in Cu_2O-AgNC on the reaction constant (K) of the reduction reaction of Congo red with excited electrons. When the Cu content in Cu_2O-AgNC increases, the reaction constant of Congo red reduction increases. However, this trend of increasing the reaction constants slows down with the increase of Cu content, because the high Cu content indicates that the thicker Cu_2O layer and on AgNC, resulting in increasing the diffusion barrier for CR molecule in nanocomposite.

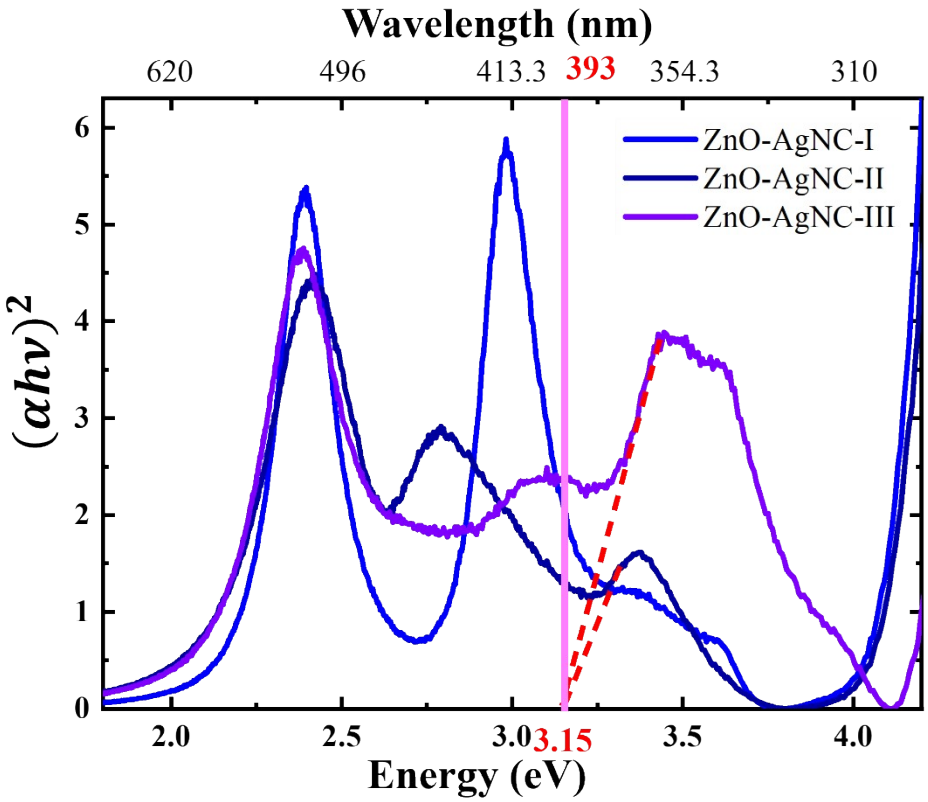

Figure S18 The energy gap of ZnO-AgNC nanocrystals can be calculated by $(\alpha hv)^2$-energy plot. ZnO-AgNC nanocrystals with different Zn contents showed an energy gap of about 3.15 eV, corresponding to 393 nm ultra-violet light. And the absorption curves (blue curve) of nanocrystals with lower ZnO content originates from the overlap between the plasmonic resonance peak of AgNC and the band gap absorption of ZnO, which make it impossible to predict the energy gap of ZnO using $(\alpha hv)^2$-energy plot.

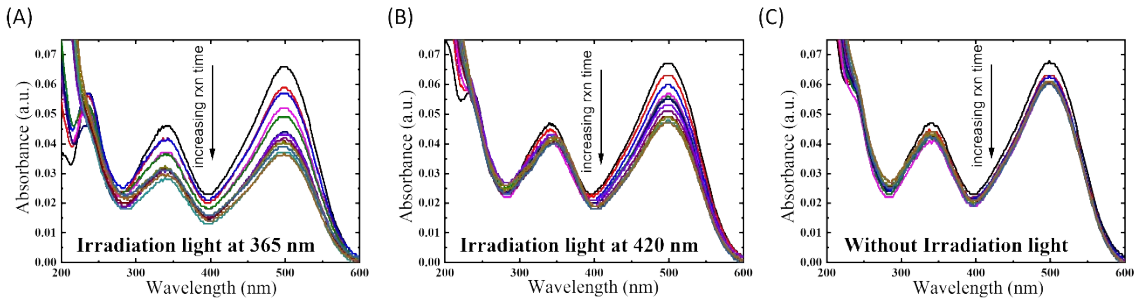

Figure S19 ZnO-AgNC nanocrystals with Zn content 1.3 atomic% were used as photocatalysts to reduce Congo red reduction under different irradiation. Changes in the Uv-Vis spectra of Congo red solution during reduction under irradiation light at (A) 365 nm, and (B) 420 nm compared to non-irradiation (C).

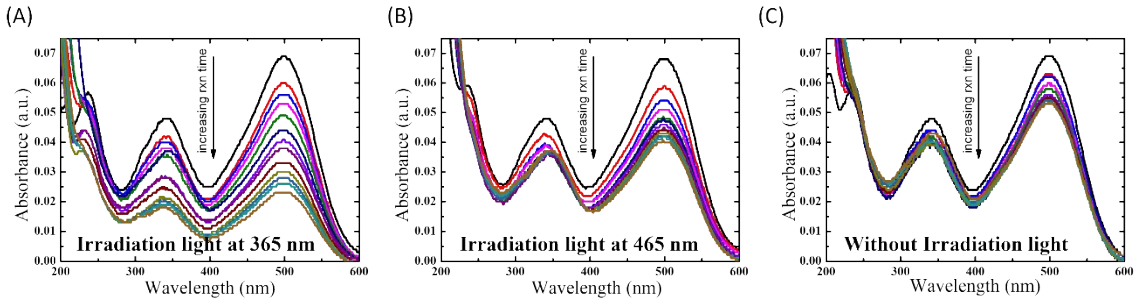

Figure S20 ZnO-AgNC nanocrystals with Zn content 9.6 atomic% were used as photocatalysts to reduce Congo red reduction under different irradiation. Changes in the Uv-Vis spectra of Congo red solution during reduction under irradiation light at (A) 365 nm, and (B) 465 nm compared to non-irradiation (C).

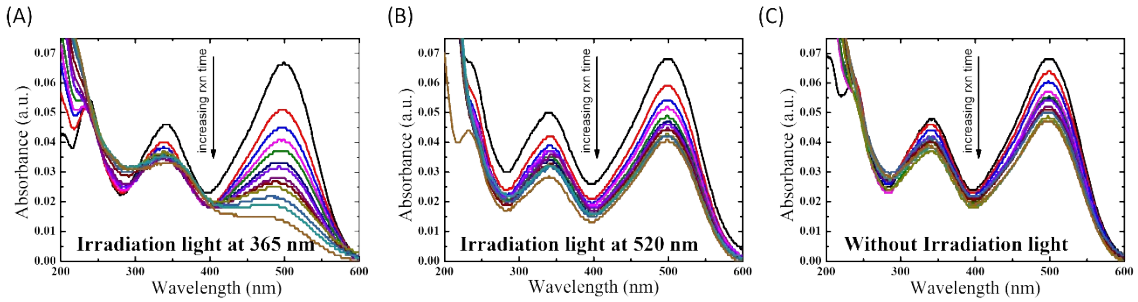

Figure S21 ZnO-AgNC nanocrystals with Zn content 25.7 atomic% were used as photocatalysts to reduce Congo red reduction under different irradiation. Changes in the Uv-Vis spectra of Congo red solution during reduction under irradiation light at (A) 365 nm, and (B) 520 nm compared to non-irradiation (C).

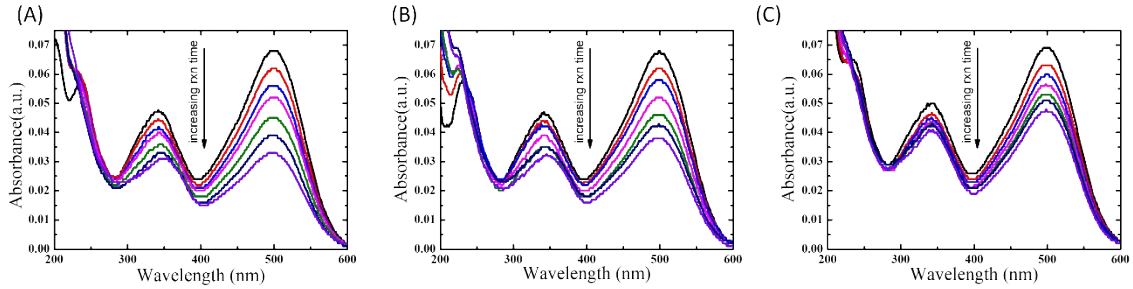

Figure S22 Different nanocrystals as photocatalysts to reduce Congo red reduction under irradiation at 410~590 nm. Changes in the Uv-Vis spectra of Congo red solution during reduction used ZnO/Cu_2O-AgNC nanocrystals (Cu content 11.6 atomic% and Zn content 7.8%) as catalysts in (A), Cu_2O/AgNC nanocrystal (Cu content 16.3 atomic%) in (B), and Zn-AgNC nanocrystal (Zn content 9.6 atomic%) as catalysts in (C).

Reference: 100 mg Cu_2O

$$Weight \times \frac{1}{Mw} \times 6.02 \times 10^{23} = \#$$

$$100\ mg \times 0.001\ \frac{g}{mg} \times \frac{1}{143.1}\ \frac{mol}{g} \times 6.02 \times 10^{23}\ \frac{\#}{mol} = 4.21 \times 10^{20}\ \#\ of\ Cu_2O$$ for 0.01435 mmol CR

→ $3.4*10^{-23}$ mmol CR / # of Cu_2O

Intensity of AgNC = 0.7 → surface coverage % of AgNC on substrate (SC%) = 16.32%

$$\#\ of\ substrate \times Area\ of\ substrate \times SC\% \div Area\ of\ AgNC = \#\ of\ AgNC$$

$$2\ substrates \times 10^{14}\ nm^2 \times 0.1632 \div 100^2\ \frac{\#\ of\ AgNC}{nm^2} = 3.264 \times 10^9\ \#\ of\ AgNC$$

$$\#\ of\ AgNC \times Volume\ of\ AgNC \times Density\ of\ Ag \times \frac{1}{Mw_{Ag}} \times 6.02 \times 10^{23} = \#\ of\ Ag$$

$$3.264 \times 10^9 \times 10^{-15}\ cm^3 \times 10.49 \frac{g}{cm^3} \times \frac{1}{107.868}\ \frac{mol}{g} \times 6.02 \times 10^{23}\ \frac{\#}{mol} = 3.174 \times 10^{16}\ \#\ of\ Ag$$

$$3.174 \times 10^{16} \times \frac{11.6/2}{54.2}\ \frac{Cu_2O\ atom\ \%}{Ag\ atom\ \%}(EDS) = 3.397 \times 10^{15}\ \#\ of\ Cu_2O$$ for 0.0001 mmol CR

→ $2.2*10^{-20}$ mmol CR / # of Cu_2O

$$3.174 \times 10^{16} \times \frac{7.8}{54.2}\ \frac{ZnO\ atom\ \%}{Aa\ atom\ \%}(EDS) = 4.568 \times 10^{15}\ \#\ of\ ZnO$$

Figure S23 Calculation and compare the number of nanocrystals for treatment the same amount of Congo red molecules. (A) free disperse Cu2O nanocrystals in an aqueous solution. (B) Cu2O-ZnO-AgNC fixed on a polymer matrix.

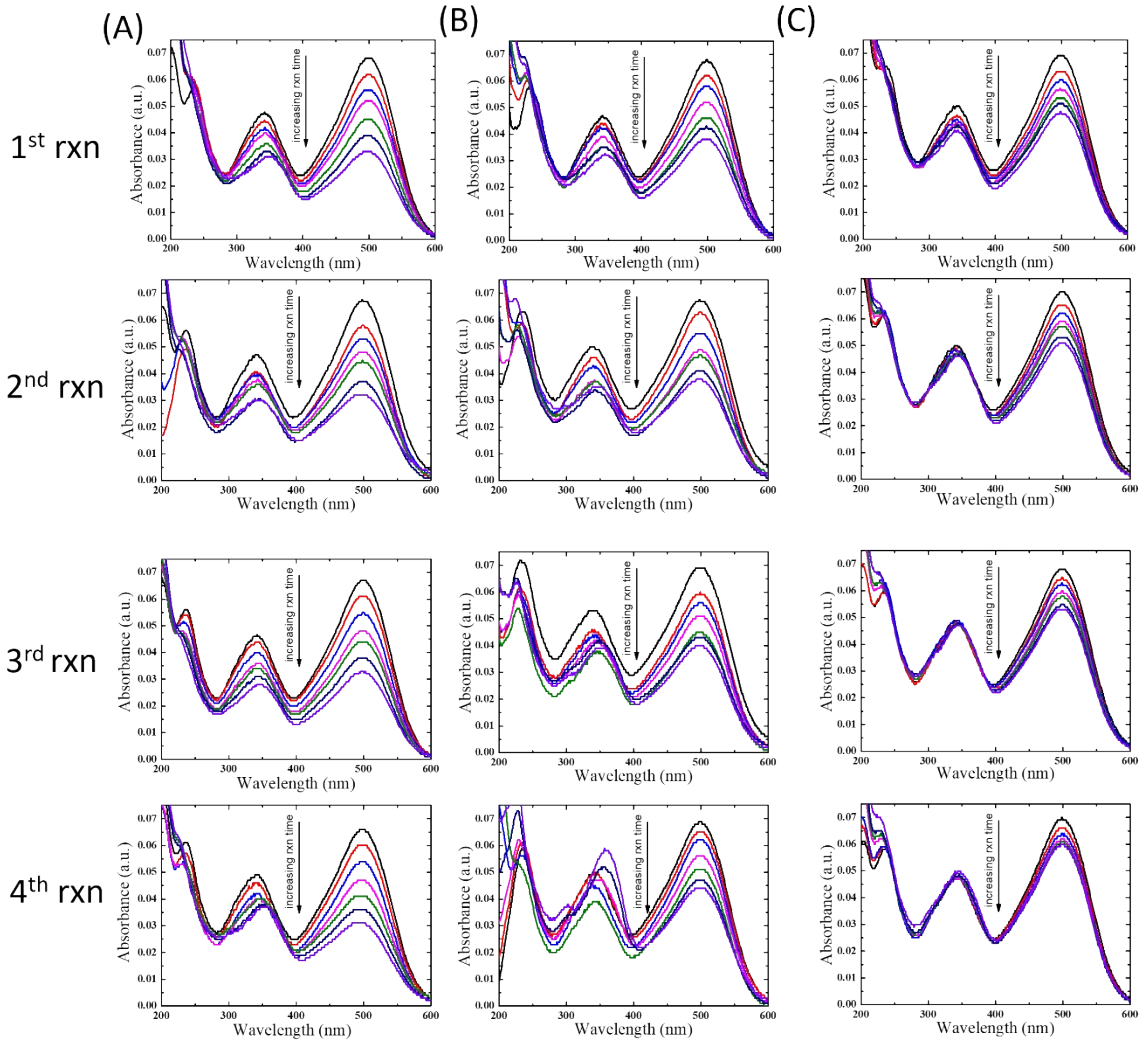

Figure S24 Stability test of three nanocrystals as catalysts for the reduction of Congo red. Changes in the Uv-Vis spectra of Congo red solution during multiple reduction reactions (1-4 cycle reaction) used ZnO/Cu_2O-AgNC nanocrystals (Cu content 11.6 atomic% and Zn content 7.8%) as catalysts in (A), Cu_2O/AgNC nanocrystal (Cu content 16.3 atomic%) (B), and Zn-AgNC nanocrystal (Zn content 9.6 atomic%) as catalysts in in (C).

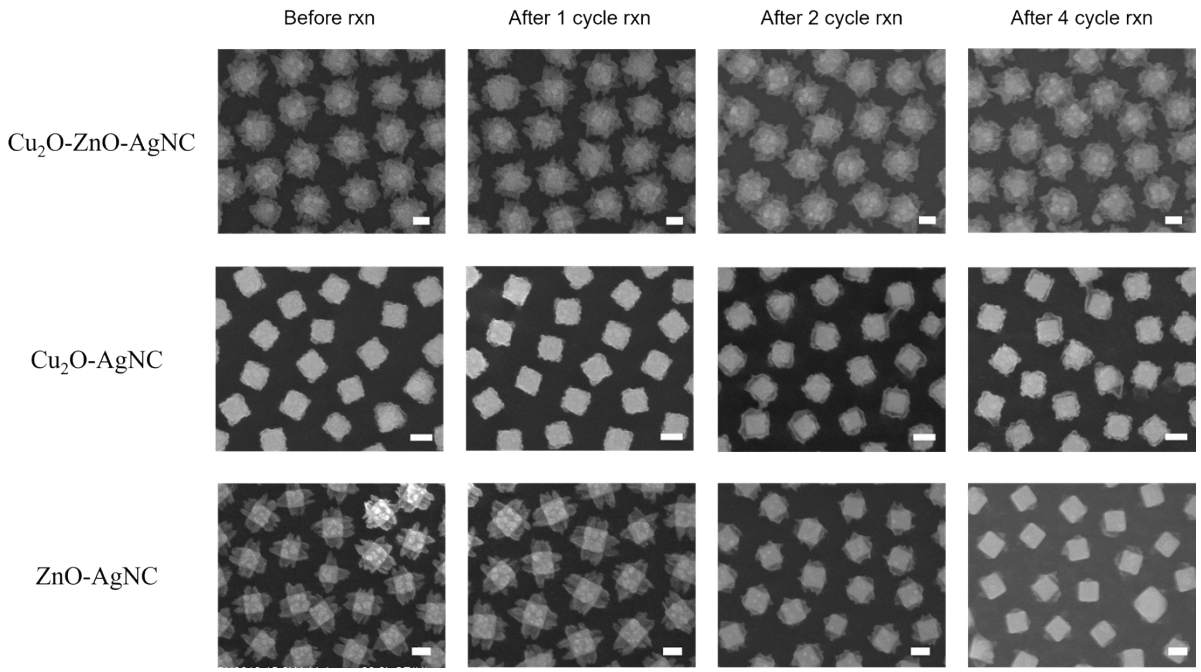

Figure S25 Stability test of three nanocrystals as catalysts for the reduction of Congo red. Changes in the morphologies of nanocrystals during multiple reduction reactions (1, 2, 4 cycle reaction) can be observed by SEM images. The scale bar is 100 nm.

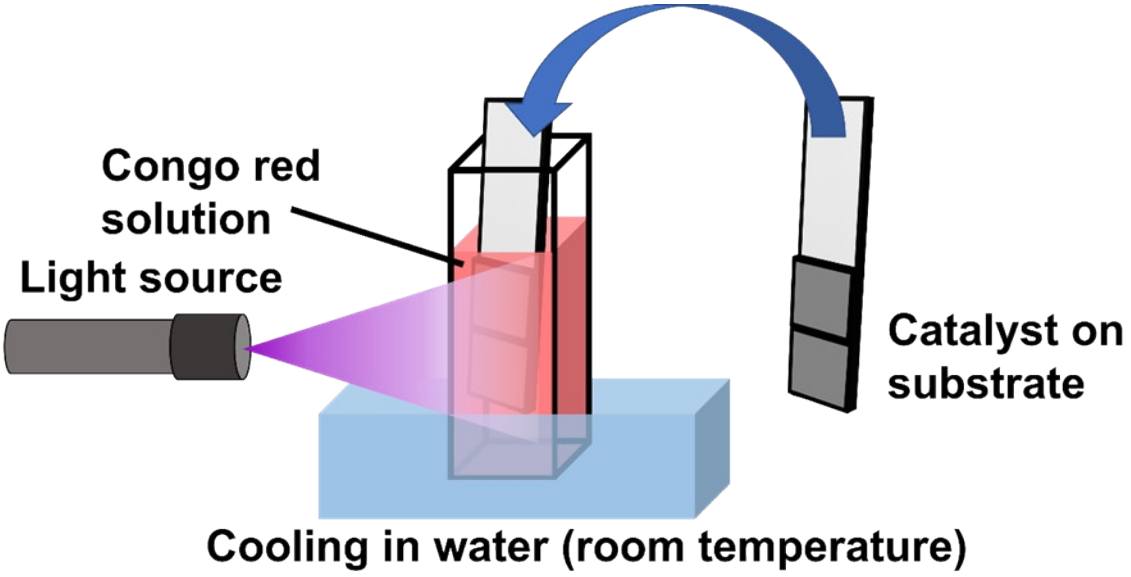

Figure S26 The schematic of reaction equipment setting up which includes the Congo red aqueous solution in a quartz cuvette. Hot-electrons are then formed on AgNC and excited electron-hole pairs on Cu_2O and/or ZnO under external irradiation.

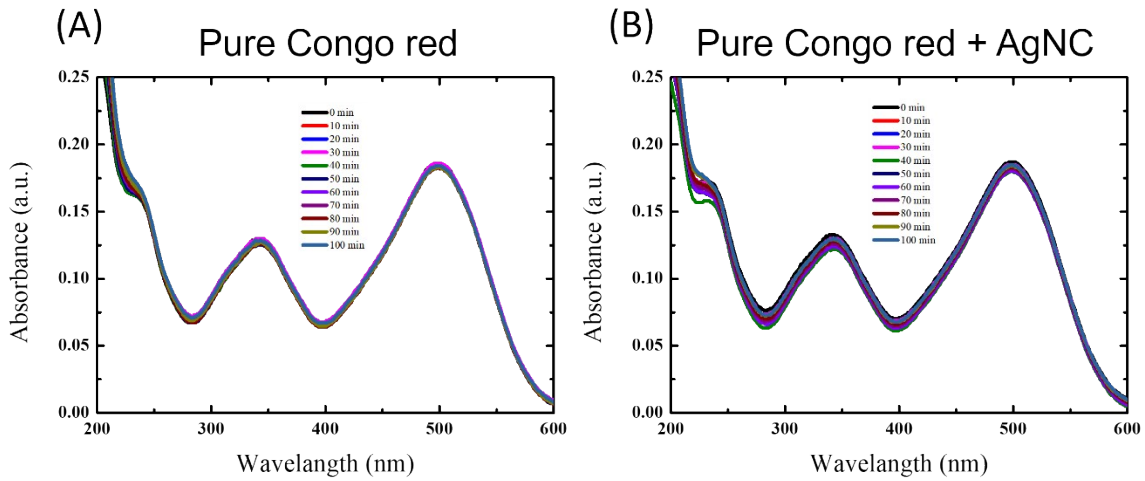

Figure S27 Photodegradation behavior of Congo red without catalysts. (A) Use the absorption spectrum of pure Congo red to observe the change in Congo red concentration under irradiation. The results showed that the concentration of Congo red did not change with time, indicating that Congo red does not undergo photodegradation in the absence of catalysts. (B) The absorption spectra of Congo red under irradiation in the presence of AgNCs also shows no change in Congo red concentration over time, indicating that AgNC is not an active material for Congo red degradation.